



# Reconstruction of fault slip of the September 21st, 1999, Taiwan earthquake in the asphalted surface of a car park, and co-seismic slip partitioning

Jacques Angelier<sup>a,\*</sup>, Jian-Cheng Lee<sup>b</sup>, Hao-Tsu Chu<sup>c</sup>, Jyr-Ching Hu<sup>d</sup>

<sup>a</sup>*Séismotectonique et Tectonophysique, ESA 7072, Université Pierre et Marie Curie, Boîte 129, 4 place Jussieu, F-75252, Paris Cedex 05, France*

<sup>b</sup>*Institute of Earth Sciences, Academia Sinica, P.O. Box 1-55, Nankang, Taipei, Taiwan, ROC*

<sup>c</sup>*Institute for Secondary School Teachers of Taiwan, Fengyuan, Taichung, Taiwan, ROC*

<sup>d</sup>*Central Geological Survey, P.O. Box 968, Taipei, Taiwan, ROC*

Received 27 May 2001; accepted 5 March 2002

## Abstract

The deformation in the asphalted surface of a car park near Wufeng ( $24^{\circ}1'N$ ,  $120^{\circ}41'E$ ) reveals the three-dimensional behaviour of the surface rupture of the September 21st, 1999, Taiwan earthquake. The N–S striking fault dips  $30^{\circ}E$  and is reverse, almost dip-slip. It accounts for about one half of the total NW–SE shortening of the whole fault zone. The remaining deformation occurred inside the upthrust block, in a damaged zone less than 3 km wide, and is dominated by N–S left-lateral shear. This distribution of co-seismic deformation highlights fault slip partitioning along an oblique fault zone, at a depth shallower than 1.7 km.

© 2002 Elsevier Science Ltd. All rights reserved.

**Keywords:** Earthquake; Rupture trace; Surface fault; Fault slip; Partitioning; Taiwan

## 1. Introduction

Roberts (2000) described pull-apart stepover structures in an asphalted road surface as ‘a geological curiosity’, and thus drew attention to the potential of such artificial layers to record ground deformation. Two other papers illustrated the reconstruction of co-seismic deformation in orientation and amplitude, based on analyses of man-made surfaces. In the first case (Angelier and Bergerat, 2002), the surface traces of the June 21st, 2000, earthquake ( $M_w = 6.4$ ) in southern Iceland, were analysed in a car park. Because the deformation was pure strike-slip, planar geometry was sufficient to fully reconstruct the co-seismic deformation. In the second case (Angelier et al., 2002), three-dimensional geometry allowed complete determination of the deformation that affected the elliptic run tracks of a stadium during the September 21st, 1999, Taiwan earthquake ( $M_w = 7.6$ ). It was aimed at discussing the methods and evaluating the uncertainties through several independent determinations of co-seismic slip. The present paper aims at quantifying slip partitioning along the same earthquake fault.

The Chichi earthquake has been studied by seismologists (Central Weather Bureau, 1999; Chung and Shin, 1999; Institute of Earth Sciences, Academia Sinica, 1999; Ma et al., 1999; Kao and Chen, 2000) and geologists (Central Geological Survey, 1999; Angelier et al., 2001; Lee et al., 2001). The surface rupture is nearly 100 km long. The motion was of thrust type with left-lateral component. This earthquake induced slip on the Chelungpu Fault (Fig. 1a). This fault is the westernmost deep thrust of the belt (the thrust to the west only affects the Late Cenozoic sediments beneath the Taichung piggyback basin). In the days following the earthquake, we analysed the rupture trace in a car park near Wufeng (latitude  $24^{\circ}1.225'N$ , longitude  $120^{\circ}41.305'E$ ), located in Fig. 1b and mapped in Fig. 2.

In this paper, we show that the local co-seismic displacement of the September 21st, 1999, earthquake in central-west Taiwan can be entirely described in three dimensions in a simple way. The determination is based on geometrical analysis in the asphalted surface of a car park cut by the rupture trace of the N–S-trending Chelungpu Fault. We also determine the proportion of total motion absorbed by the fault slip, based on the comparison between our determination on the rupture trace and the far field information provided by geodetic analyses.

\* Corresponding author. Fax: +33-1-44-27-50-85.

E-mail address: jacques.angelier@lgs.jussieu.fr (J. Angelier).

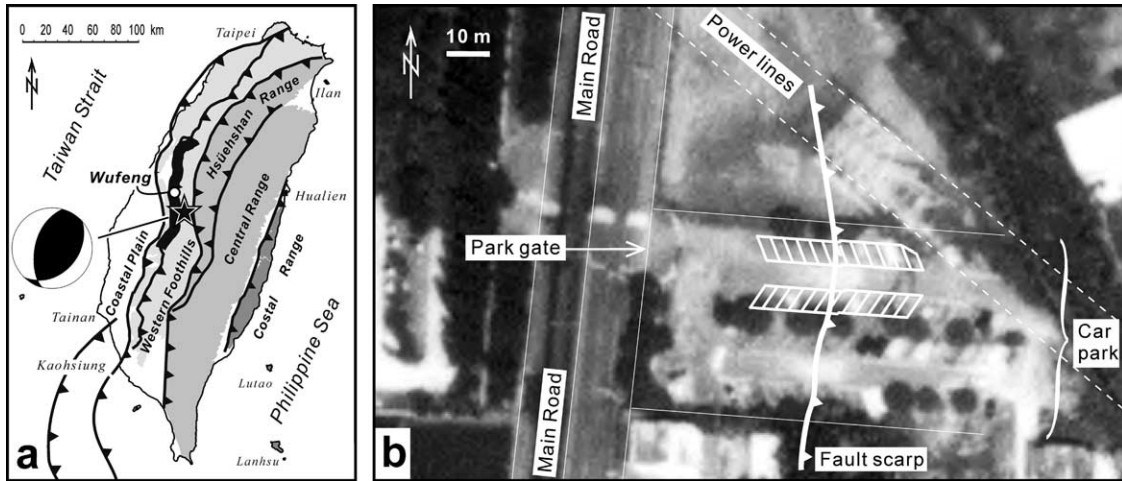


Fig. 1. (a) Location of the site studied (open dot) in Taiwan. September 21st, 1999 earthquake with epicentre as star, rupture trace as thick black line and focal mechanism as beachball-type stereoplot. Main thrusts of the Taiwan belt with triangles on upthrust side. (b) Aerial view of Wufeng car park. Area of Fig. 2 shown with white lines bounding parking lots.

**2. Geometrical analysis of co-seismic faulting in the car park**

Two rows of the car park are mapped in Fig. 2a. They strike N94°E and were crosscut by the N4°E-trending fault scarp of the earthquake. The fracture zone is 3–6 m wide in the hanging wall, and a minor rupture occurs

10–20 m east of the main fault (Fig. 2a). The narrow fault scarp is  $1.62 \pm 0.06$  m high (Fig. 2b). The reverse nature of co-seismic faulting is illustrated by gaps in the sequences of painted numbers, revealing missing park lots (Fig. 3).

The rows were analysed separately; the results were identical within the range of uncertainties. In the N94°E

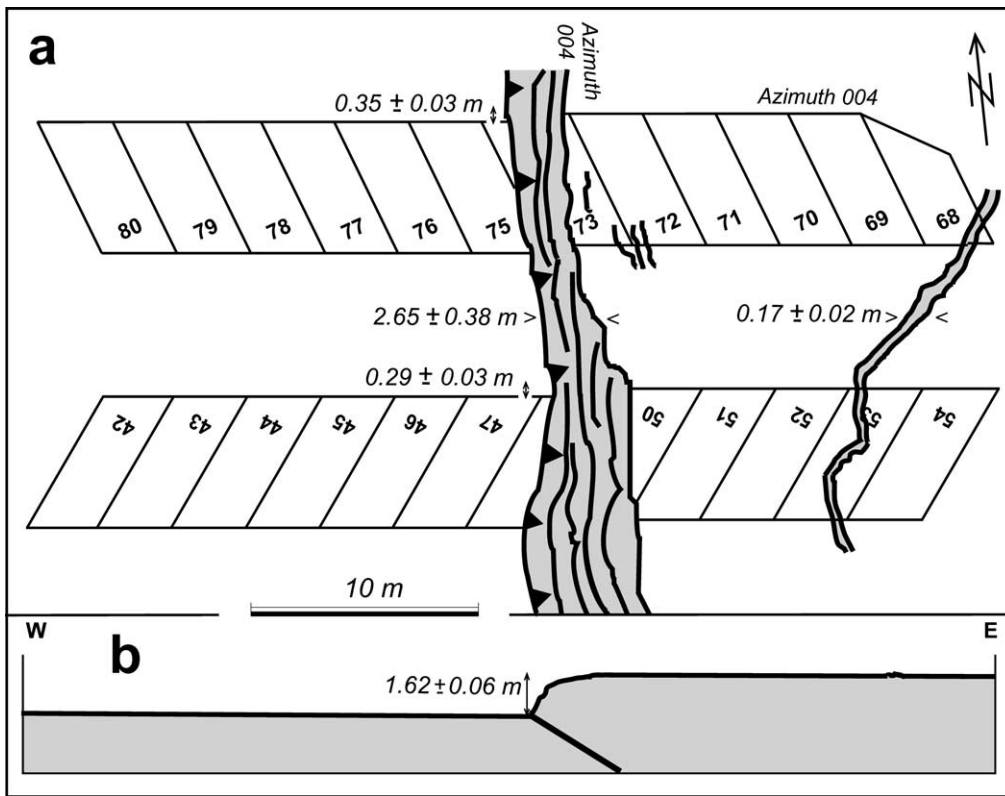


Fig. 2. Map (a) and topographic profile (b) of the Wufeng car park (northern two rows). Fracture zones in grey, main fault with triangles on upthrust side. Note missing park lots.

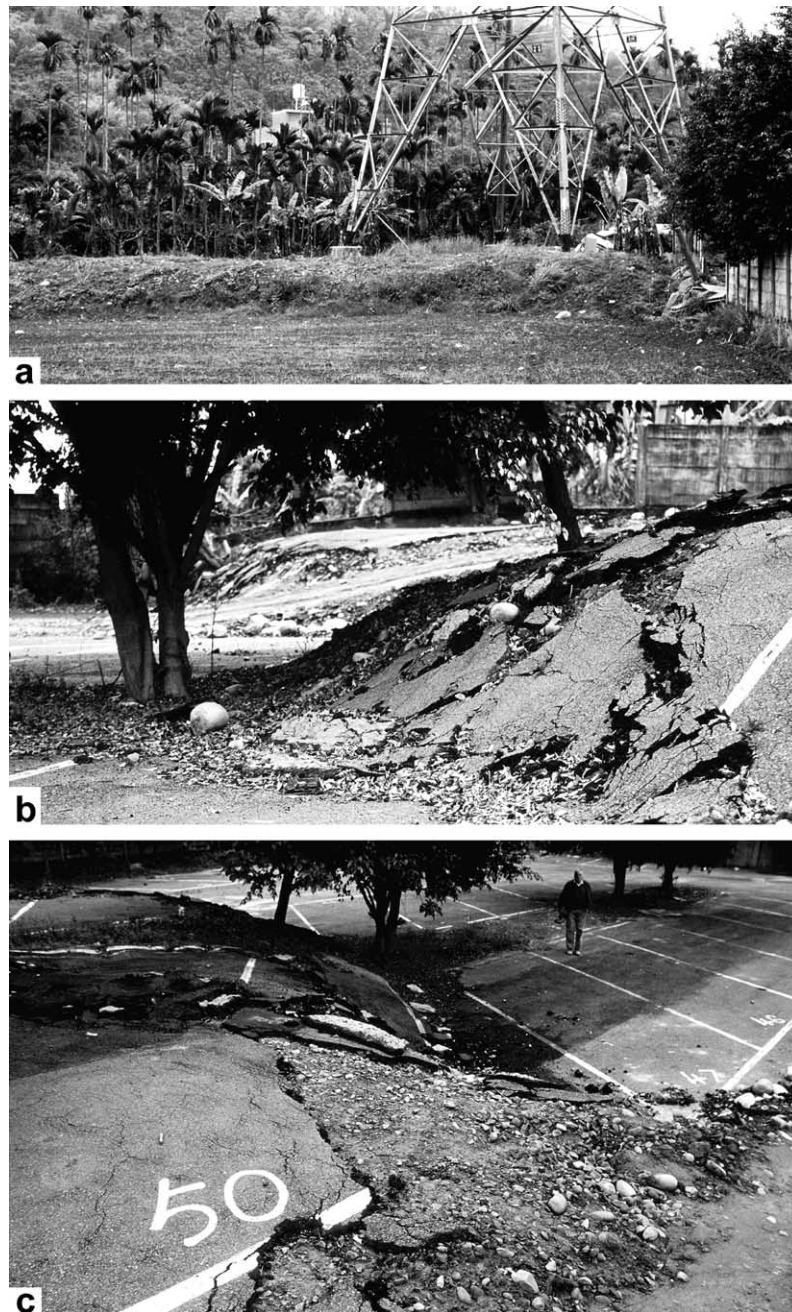


Fig. 3. The N–S-trending rupture trace at the Wufeng car park. (a) Fault scarp, view to the east, northern wall of car park on right. (b) View to the north, fault scarp cutting across rows 42–54 (foreground) and 68–80 (background), compare with Fig. 2. (c) View to the southwest; the width of park lots 48–49 (missing numbers between 47 and 50) is 60% of the original width.

direction, we measured the width of the 17 park lots left intact by faulting (Fig. 2a). The average value and standard deviation,  $3.24 \pm 0.03$  m, show that the park lots were almost identical in width. Before the earthquake, each row included 13 lots, so that the total width was  $42.12 \pm 0.39$  m. The corresponding distance measured after the earthquake is  $39.30 \pm 0.01$  m. The co-seismic horizontal shortening in the N94°E direction is the difference between these values,  $2.82 \pm 0.40$  m. The contribution of the minor rupture is 0.17 m. The row-perpendicular

offset is  $0.32 \pm 0.03$  m, left-lateral, in the N4°E direction (Fig. 2a).

Because the fault scarp trends N4°E, the relative displacements perpendicular and parallel to the N94°E-trending row directly yield the strike-slip and the horizontal transverse components of fault slip. With a vertical offset of  $1.62 \pm 0.06$  m, a transverse horizontal component of slip of  $2.82 \pm 0.40$  m and a left-lateral component of  $0.32 \pm 0.03$  m (Fig. 2), other values are calculated using the Pythagorean theorem for distances and tangents for

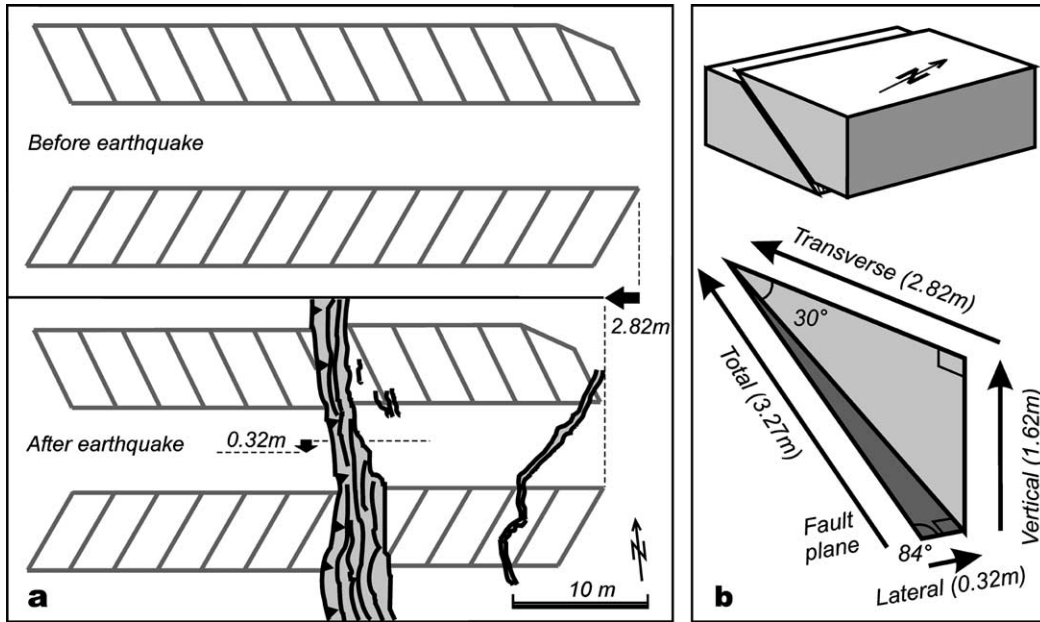


Fig. 4. Geometry of co-seismic fault slip, Wufeng car park. (a) Map view of E–W shortening and N–S left-lateral offset. (b) Fault attitude and components of relative displacement.

angles. The total slip is  $3.27 \pm 0.38$  m. The dip-slip component is similar ( $3.25 \pm 0.38$  m). The left-lateral and dip-slip components indicate the pitch of the slip vector,  $84 \pm 1^\circ$  towards the south. The vertical and transverse horizontal components indicate a fault dip angle of  $30 \pm 5^\circ$  towards the east (Fig. 4). The reverse dip-slip and left-lateral components of horizontal relative displacement reveal a clockwise angle of  $83 \pm 2^\circ$  from the slip direction to the  $N4^\circ E$  fault strike, giving as the trend of the slip vector  $N79^\circ W \pm 2^\circ$  (hanging wall relative to footwall). The horizontal shortening in this direction is  $2.84 \pm 0.40$  m.

### 3. Distribution of co-seismic displacement west and east of the car park

Our estimate of fault slip deserves comparison with the results of the surrounding GPS geodetic stations surveyed before and after the Chichi earthquake (Hou et al., 2000; Johnson et al., 2001; Yu et al., 2001). Eight stations are located near a WNW–ESE profile centred in the Wufeng car park (Fig. 5). Their distances to the fault are in the range 0–18 km on the footwall side, and 3–29 km on the hanging wall side. Their displacement vectors are similar in azimuth,

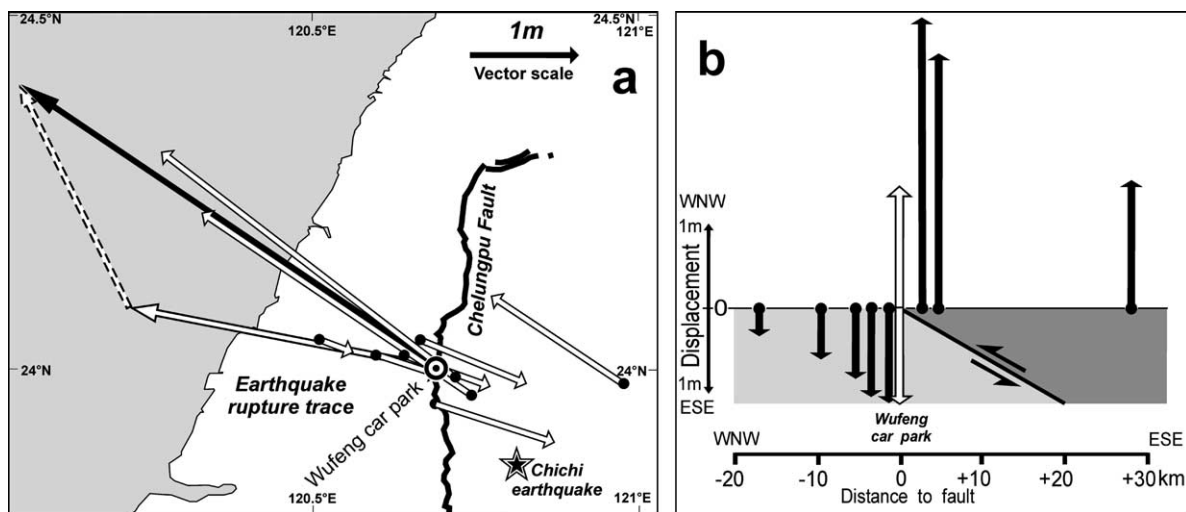


Fig. 5. Horizontal components of fault slip and far-field deformation of Chichi earthquake, Wufeng car park region. (a) Comparison between relative displacements on fault trace (large open arrow) and across a 3-km-wide zone including fault (solid arrow). Vector difference as dashed open arrow. GPS displacement data from Hou et al. (2000) and Yu et al. (2001), with eight selected stations as black dots and vectors as open arrows. (b) Components of horizontal displacement along a  $N118^\circ E$ -trending profile (black arrows). Same stations as in (a). Footwall and hanging wall slip components in Wufeng car park as open arrows.

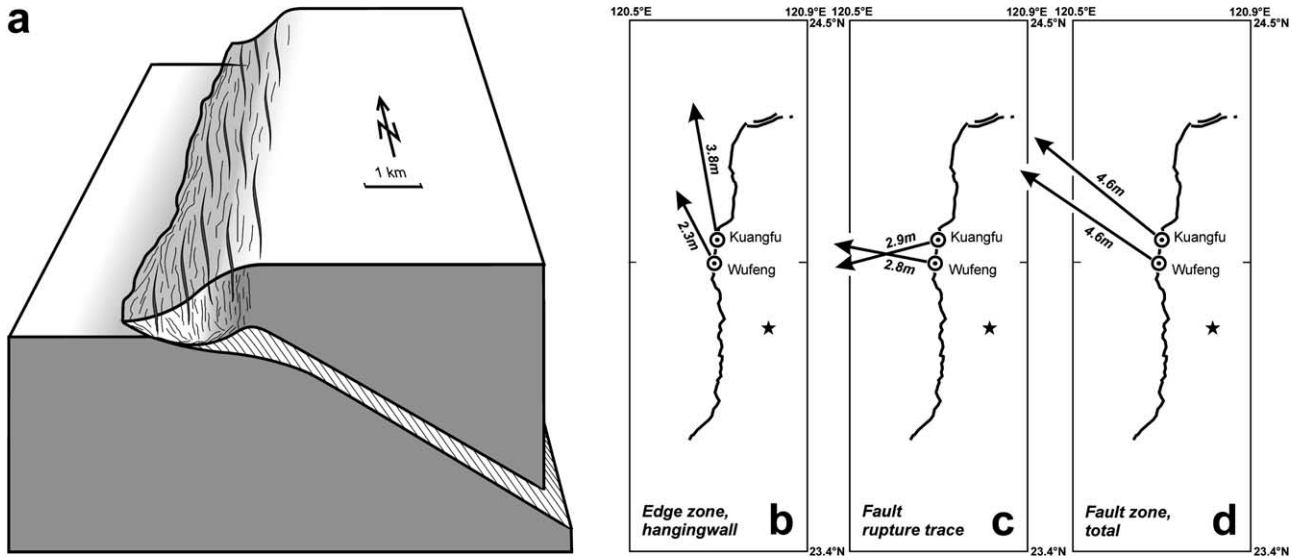


Fig. 6. Slip partitioning in the Chelungpu Fault zone. (a) Westward dip-slip thrusting prevails on rupture trace, whereas N–S distributed left-lateral shear associated with minor E–W shortening is accommodated in hanging wall by pervasive faulting, fissuring and folding. (b) Displacement of eastern boundary of the highly deformed zone relative to upthrust side of fault at Wufeng (this paper) and Kuangfu (Angelier et al., 2002), mainly accommodated by fracturing and pervasive left-lateral shear. Vector construction in Fig. 5a. Chelungpu Fault as thick black line, earthquake epicentre as star. (c) Displacement at rupture trace (hanging wall relative to footwall), same sites, with dip-slip thrusting at Wufeng and left-lateral thrusting at Kuangfu (local NW–SE fault strike not visible at map scale). (d) Total relative displacement.

about N111°E for the footwall and N55°W for the hanging wall. The average trend, N118°E, coincides with the N119°E direction of maximum compression revealed by the inversion of focal mechanisms of the Chichi earthquake sequence (Kao and Angelier, 2001).

The displacement regularly decreases away from the fault, on both the footwall and the hanging wall, which highlights the amplitude of the co-seismic elastic response (Fig. 5b). Considering the nearest footwall and hanging wall stations around the site studied, and adding their vectors, the horizontal hanging wall displacement relative to footwall is 4.60 m in the N56°W direction, that is, 3.81 m towards the west and 2.57 m towards the north (Fig. 5a).

#### 4. Discussion and conclusions

Our data collected in the car park near Wufeng indicate that the N–S earthquake fault dips 30°E (a typical dip angle for a reverse fault) and is almost pure dip-slip. This dip angle at the surface is scarcely steeper than, and generally consistent with, the 25° dip angle determined at the 5–12 km focal depth of the Chichi earthquake (Chung and Shin, 1999; Kao and Chen, 2000). Farther north, at Kuangfu, the same fault dips 40–45°E and locally strikes NW–SE (Angelier et al., 2002). The Kuangfu site is located in a sharp bend of the fault, whereas at Wufeng the rupture trace exhibits the usual N–S strike of the Chelungpu Fault. We infer that the geometrical reconstruction done in the Wufeng car park better illustrates the regional attitude of the earthquake fault (Fig. 4b). This

site should thus be regarded as typical, in the absence of major perturbation that would have affected the fault attitude near the surface.

Whereas the displacement of the hanging wall relative to footwall is 4.60 m in the N56°W direction based on the data from the nearest GPS stations, it is 2.84 m in the N79°W direction in the car park, that is, 2.79 m towards the west and 0.54 m towards the north (Fig. 5a). Not only is this amount larger, but the azimuths differ by 23°. The vector difference between the two determinations is 1.02 m towards the west and 2.03 m towards the north, that is, 2.27 m in the N27°W direction (Fig. 5a). Considering the N4°E strike of the fault, these values imply an additional transverse shortening of 1.16 m and an additional left-lateral motion of 1.96 m, with respect to our local result (2.82 and 0.34 m, respectively). Because the footwall station is close to the fault, these differences reflect deformation in the upthrust unit (Fig. 6a). Based on the position of the hanging wall station, this deformation must occur within a distance of 3 km east of the rupture trace. These GPS data also suggest that the contribution of footwall motion to shortening in the car park is less than 40%.

The horizontal component of co-seismic slip in the car park (2.84 m, N79°W) represents 2.62 m of relative displacement in the N56°W direction and thus only accounts for 57% of the motion that occurred across both the fault and the deformed hanging wall (Fig. 5a). Faulting, pervasive fissuring and folding inside this edge zone, which suffered widespread damage during the earthquake, absorbed the remaining 43%. The deformation of the hanging wall thus represents only 29% of the total fault-perpendicular

shortening, but as much as 85% of the total fault-parallel left-lateral shear. This implies that the contraction in the car park accounts for 71 and 15% of these components, respectively. This comparison shows that whereas dip-slip thrusting prevailed across the rupture trace, left-lateral strike-slip in the N–S direction dominated east of it, on the hanging wall side of the fault (Fig. 6a).

Farther north, the Kuangfu site revealed a distribution of co-seismic displacement and deformation that resembles that of the Wufeng car park, despite major differences in the local strike of the fault, NW–SE instead of N–S, and its dip angle, 45° instead of 30° (Angelier et al., 2002). With respect to the upthrust side of the fault, northward displacement prevails in both cases in the hanging wall edge zone (Fig. 6b), indicating pervasive left-lateral shear in an elongated domain less than 3–7 km wide. Displacement towards the west prevails across the rupture trace itself (Fig. 6c), indicating dip-slip thrusting at Wufeng and left-lateral thrusting at Kuangfu. The sum of these two vectors is a displacement towards the NW across the whole fault zone (Fig. 6d). That similar displacement vectors occur despite contrasting fault attitudes highlights widespread partitioning at shallow depths. The displacement on the fault trace thus reveals belt-perpendicular thrusting (Fig. 6c) rather than belt-parallel left-lateral shear (Fig. 6b), within the frame of oblique NW–SE contraction across the whole thrust zone (Fig. 6d).

The behaviour of the Chelungpu Fault during the Chichi earthquake thus provides a typical example of fault slip partitioning. At Wufeng, the highly deformed edge zone of the hanging wall, where strike-slip deformation prevails, is less than 3 km wide. With the fault dip angle of 30° determined in the car park, the maximum thickness of this deformation zone is certainly less than 1.7 km. Farther east, at larger depths, oblique slip occurs on a single fault.

### Acknowledgements

The French Institute in Taipei, the National Council of Taiwan, the ‘Institut Universitaire de France’ and the ‘Bureau de Représentation de Taiwan’ in Paris supported this study. Useful comments were made by J.P. Evans.

### References

- Angelier, J., Bergerat, F., 2002. Behaviour of a rupture of the June 21st, 2000, earthquake in South Iceland as revealed in an asphalted car park. *Journal of Structural Geology* in press (PII: S0191-8141(02)00007-X).
- Angelier, J., Lee, J.-C., Chu, H.-T., Hu, J.-C., Lu, C.-Y., Chan, Y.-C., Lin, T.-J., Font, Y., Deffontaines, B., Tsai, Y.-B., 2001. Le séisme de Chichi (1999) et sa place dans l’orogène de Taiwan. *Comptes Rendus de l’Académie des Sciences Paris II* 333 (1), 5–21.
- Angelier, J., Lee, J.-C., Hu, J.-C., Chu, H.-T., 2002. Three-dimensional deformation along the rupture trace of the September 21st, 1999, Taiwan earthquake: a case study in the Kuangfu school. *Journal of Structural Geology* in press (PII: S0191-8141(02)00039-1).
- Central Geological Survey, 1999. Surface ruptures along the Chelungpu fault during the Chi-Chi earthquake, Taiwan. Map, scale 1:25,000, Ministry of Economic Affairs, Republic of China, Taipei, 4 sheets.
- Central Weather Bureau, 1999. The Chi-Chi Earthquake in Taiwan. Internet site at address <http://www.cwb.gov.tw>.
- Chung, J.-K., Shin, T.-C., 1999. Implication of the rupture process from the displacement distribution of strong ground motions recorded during the 21 September 1999 Chi-Chi, Taiwan earthquake. *Terrestrial Atmospheric Ocean*, Taipei 10, 777–786.
- Hou, C.-S., Lai, T.-C., Fei, L.-Y., Wang, J.-S., Chen, W.-H., 2000. Highly accurate surveying in the study of the Chelungpu active fault-comparison of the data before and after the Chi-Chi Earthquake. *Central Geological Survey, Special Publication* 12, 191–210.
- Institute of Earth Sciences, Academia Sinica, 1999. The Chi-Chi Earthquake in Taiwan. Internet site at address [http://www.earth.sinica.edu.tw/921/921chichi\\_main\\_eng.htm](http://www.earth.sinica.edu.tw/921/921chichi_main_eng.htm).
- Johnson, K., Hsu, Y.J., Segall, P., Yu, S.B., 2001. Fault geometry and slip distribution of the 1999 Chi-Chi, Taiwan earthquake imaged from inversion of GPS data. *Geophysical Research Letters* 28, 2285–2288.
- Kao, H., Chen, W.-P., 2000. The Chi-Chi earthquake sequence: active out-of-sequence thrust faulting in Taiwan. *Science* 288, 2346–2349.
- Kao, H., Angelier, J., 2001. Stress tensor inversion for the Chi-Chi earthquake sequence and its implications on regional collision. *Bulletin of the Seismological Society of America* 91 (5), 1028–1040.
- Lee, J.-C., Chu, H.-T., Angelier, J., Chan, Y.-C., Hu, J.-C., Lu, C.-Y., Rau, R.-J., 2001. Geometry and structure of northern surface ruptures of the 1999 Mw = 7.6 Chi-Chi, Taiwan earthquake: influence from inherited fold belt structures. *Journal of Structural Geology* 24, 173–192.
- Ma, K.-F., Lee, C.-T., Tsai, Y.-B., Shin, T.-C., Mori, J., 1999. The Chi-Chi, Taiwan earthquake: large surface displacements on an inland thrust fault. *EOS Transactions* 80, 605–611.
- Roberts, D., 2000. Pull-apart stepover structures in an asphalted road surface—a geological curiosity. *Journal of Structural Geology* 22, 1469–1472.
- Yu, S.-B., Kuo, L.-C., Hsu, Y.-J., Su, H.-H., Liu, C.-C., Hou, C.-S., Lee, J.-F., Lai, T.-C., Liu, C.-C., Liu, C.-L., Tseng, T.-F., Tsai, C.-S., Shin, T.-C., 2001. Preseismic deformation and coseismic displacements associated with the 1999 Chi-Chi, Taiwan, Earthquake. *Bulletin of the Seismological Society of America* 91 (5), 995–1012.